Band-structure topologies of graphene: Spin-orbit coupling effects from first principles

M. Gmitra,[1] S. Konschuh,[1] C. Ertler,[1] C. Ambrosch-Draxl,[2] and J. Fabian[1]
[1]*Institute for Theoretical Physics, University of Regensburg, 93040 Regensburg, Germany*
[2]*Chair of Atomistic Modeling and Design of Materials, University of Leoben, Franz-Josef-Strasse 18, 8700 Leoben, Austria*
(Received 26 November 2009; published 28 December 2009)

The electronic band structure of graphene in the presence of spin-orbit coupling and transverse electric field is investigated from first principles using the linearized augmented plane-wave method. The spin-orbit coupling opens a gap of 24 μeV (0.28 K) at the $K(K')$ point. It is shown that the previously accepted value of 1 μeV, coming from the σ-π mixing, is incorrect due to the neglect of d and higher orbitals whose contribution is dominant due to symmetry reasons. The transverse electric field induces an additional (extrinsic) Bychkov-Rashba-type splitting of 10 μeV (0.11 K) per V/nm, coming from the σ-π mixing. A "miniripple" configuration with every other atom shifted out of the sheet by less than 1% differs little from the intrinsic case.

DOI: 10.1103/PhysRevB.80.235431 PACS number(s): 71.15.Mb, 31.15.aj, 31.15.es, 71.90.+q

The fascination with graphene,[1] the one-atom-thick allotrope of carbon, comes from its two-dimensional structure as well as from its unique electronic properties.[2–7] The latter originate from the specific electronic band structure at the Fermi level: electrons move with a constant velocity, apparently without mass and a spectral gap. Analogy with massless Dirac fermions is often drawn, presenting graphene as a solid-state toy for relativistic quantum mechanics. Ironically, this nice analogy is broken by the relativistic effects themselves. In particular, the interaction of the orbital and spin degrees of freedom, spin-orbit coupling, gives the electrons in graphene a finite mass and induces a gap in the spectrum. How large is the gap and which orbital states contribute to it? This question is crucial for knowing graphene's band-structure topology, understanding its spin transport and spin relaxation properties,[8,9] or for assessing prospects of graphene for spin-based quantum computing.[10] By performing comprehensive first principles calculations we predict the spectral gap and establish the relevant electronic spectrum of graphene in the presence of external transverse electric field. We find that realistic electric fields can tune among different band structure topologies with important ramifications for the physics of graphene.

Carbon atoms in graphene are arranged in a honeycomb lattice which comprises two triangular Bravais lattices; the unit cell has two atoms. The corresponding reciprocal lattice is again honeycomb, with two nonequivalent vertices K and K' which are the Fermi momenta of a neutral graphene. The states relevant for transport are concentrated in two touching cones with the tips at $K(K')$—the Dirac points—as illustrated in Fig. 1. The corresponding Bloch states are formed mainly by the carbon valence p_z orbitals (the z axis is perpendicular to the graphene plane) forming the two π bands (cones). The other three occupied valence states of carbon form the deep-lying σ bands by sp^2 hybridization; these are responsible for the robustness of graphene's structure. The states in the lower cones are holelike or valencelike, while the upper cone states are electronlike or conductionlike, borrowing from semiconductor terminology. These essentials of the electronic band structure of graphene were worked out many decades ago.[11–16]

The above picture breaks down when spin-orbit coupling is included. The most important modification to the band structure is the opening of a gap at $K(K')$. The magnitude of this gap has been believed to be 1 μeV, requiring very low temperatures (0.01 K) to probe. This estimate comes from the σ-π mixing, rescaling down (to the second order) the spin-orbit splitting of the p states in the carbon atom which is on the order of 10 meV. However, as predicted already by Slonczewski,[15,17] it is the d orbitals and higher that give dominant contributions (in the first order of the respective atomic splittings); the σ-π mixing, on which previous investigations focused, should be negligible. This is indeed what we find from first principles. The gap jumps from 1 to 24 meV upon switching on d and higher orbitals, making it accessible at temperatures of 0.2 K. More severe changes occur when graphene is subject to transverse electric fields that can come from the substrate or electric gates. We explore, from first principles, the fascinating spectral topologies around the $K(K')$ points, extracting the electrical field induced (Bychkov-Rashba) spin-orbit splitting of 10 μeV (0.11 K) per V/nm; we prove that this splitting is dominated by the σ-π mixing only. To investigate the electronic band structure of graphene in the presence of spin-orbit coupling

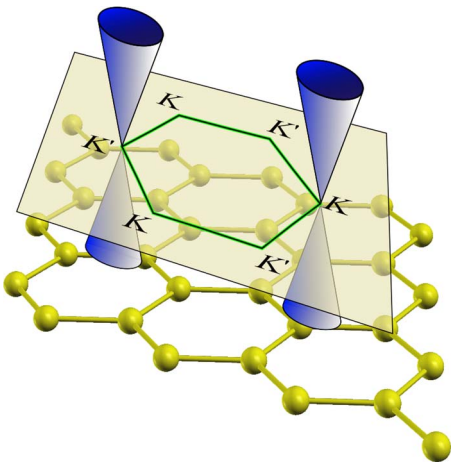

FIG. 1. (Color online) Graphene's essentials. Bottom-up: carbon atoms form a honeycomb lattice with two atoms in the unit cell. The first Brillouin zone of the reciprocal lattice contains two nonequivalent Dirac points, K and K'. The relevant states at the Fermi level form two touching cones with the tips at $K(K')$.

 ©2009 The American Physical Society

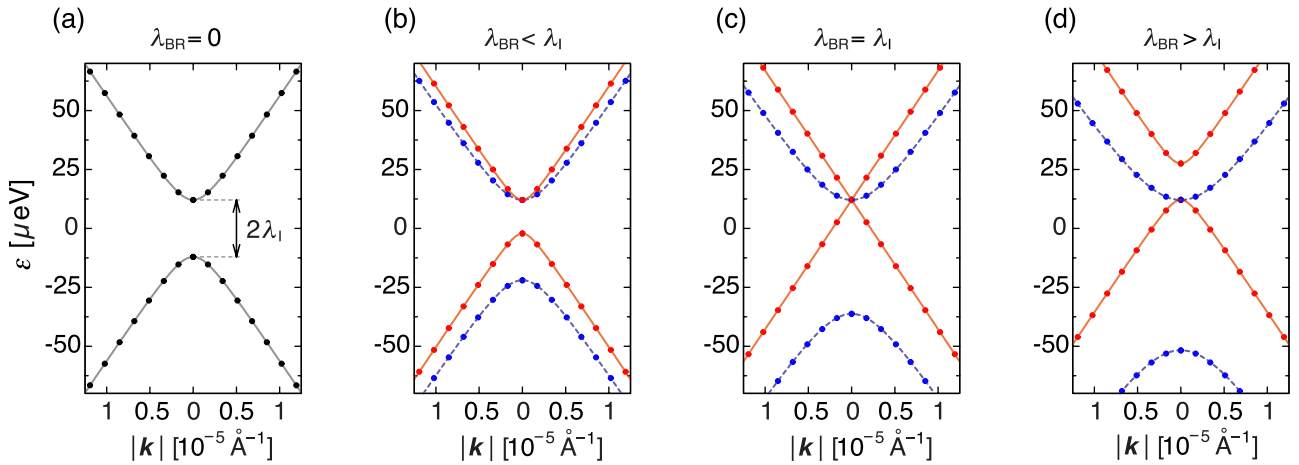

FIG. 2. (Color online) Band-structure topologies of graphene. Transverse electric field drastically changes the topology of the bands near $K(K')$. (a) Zero electric field. (b) Electric field of magnitude $E=1.0$ V/nm. (c) $E=2.44$ V/nm. (d) $E=4.0$ V/nm. The first principles results are represented by circles (the Fermi level is at zero). The curves are fits to the analytical model. The spin branch $\mu=1$ is shown in solid (red), $\mu=-1$ in dashed (blue). The calculated Fermi velocity is $v_F=0.833\times10^6$ m/s.

we employed the full potential linearized augmented plane wave (LAPW) method based on density functional theory.[18] For exchange-correlation effects we used the generalized gradient approximation.[19] In our three-dimensional calculation the graphene sheets of lattice constant $a=1.42\sqrt{3}$ Å are separated by the distance 20 Å, large enough for the intersheet tunneling to be negligible. Integration in the reciprocal space was performed by the modified Blöchl tetrahedron scheme, taking the mesh of 33×33 k points in the irreducible Brillouin zone wedge. As the plane-wave cutoff we took 9.87 Å^{-1}. The $1s$ core states were obtained by solving the Dirac equation, while spin-orbit coupling for the valence electrons was treated within the muffin-tin radius of 1.34 a.u. by the second variational method. Finally, external transverse electric field was included as a periodic zigzag electric potential added to the exchange-correlation functional.[20]

Our main results are shown in Fig. 2 which displays a variety of the band structure topologies of graphene, tunable by electric field. The intrinsic case (zero external field) shows a splitting of the Dirac cones at the $K(K')$ points into two "rounded" cones, with the gap of $2\lambda_I=24$ μeV (0.28 K). The bands are twofold degenerate due to the presence of time reversal and space inversion symmetries.[21] Transverse electric field breaks the latter symmetry, resulting in a spin-splitting $2\lambda_{BR}$ of the energy levels: for each momentum at a given band there are two states with energy differing by $2\lambda_{BR}$. This extrinsic splitting is akin to the Bychkov-Rashba (BR) spin-orbit coupling in semiconductor heterostructures.[22]

The band structure of graphene in the presence of transverse electric field depends rather strongly on the interplay of the intrinsic and extrinsic spin-orbit coupling effects. As the magnitude of the electric field increases, we encounter the topologies on display in Fig. 2. If the BR splitting is lower than the intrinsic one, the spectral gap gets smaller. The electron branch of the spectrum is still degenerate at $K(K')$; in contrast, the hole branch is split by $2\lambda_{BR}$. This topology can give a quantum spin Hall insulator.[9] Curiously, as the electric field is such that $\lambda_{BR}=\lambda_I$, one of the hole branches rises, forming a genuine touching cones structure of massless fermions with one of the electron branches. The two remaining branches are parabolic (massive). For fields such that $\lambda_{BR}>\lambda_I$, all the branches are again parabolic, with a degeneracy of one electron and one hole band. The calculated spectrum at $K(K')$ follows the recipe $\mu\lambda_{BR}+\nu|\lambda_{BR}-\mu\lambda_I|$, with μ and ν being ±1.

The physics behind the calculated spectral topologies can be described qualitatively by previously proposed effective Hamiltonians. Without spin-orbit coupling the electronic band structure of graphene in the vicinity of $K(K')$ is described by the Hamiltonian $\mathcal{H}_0=\hbar v_F(\kappa\sigma_x k_x+\sigma_y k_y)$. Here v_F is the Fermi velocity, k_x and k_y are the Cartesian components of the electron wave vector measured from $K(K')$, the parameter $\kappa=1(-1)$ for the cones at $K(K')$, and σ_x and σ_y are the Pauli matrices acting on the so called pseudospin space formed by the two triangular sublattices of graphene. The Hamiltonian $\mathcal{H}_0$ describes gapless states with conical dispersion $\varepsilon_0=\nu\hbar v_F|\boldsymbol{k}|$ near the Dirac points. The eigenstates are $\psi_\nu=1/\sqrt{2}|\nu e^{-i\kappa\varphi},1\rangle$ for the electron band, $\nu=1$, and hole band, $\nu=-1$, and $\tan\varphi=k_y/k_x$.

The intrinsic spin-orbit coupling is described by the effective Hamiltonian $\mathcal{H}_{SO}=\lambda_I\kappa\sigma_z s_z$.[9,16] Here s_z is the spin Pauli matrix. The spin-orbit coupling lifts the orbital degeneracy at $K(K')$. Indeed, the eigenvalues of the combined Hamiltonian, $\mathcal{H}_0+\mathcal{H}_{SO}$, are $\varepsilon_\nu=\nu\sqrt{\varepsilon_0^2+\lambda_I^2}$. The bands are split by $2|\lambda_I|$, but the twofold degeneracy of the bands, required by space inversion and time reversal symmetry, remains.

The extrinsic spin-orbit coupling of the Bychkov-Rashba type in graphene can be described by the Hamiltonian $\mathcal{H}_{BR}=\lambda_{BR}(\kappa\sigma_x s_y-\sigma_y s_x)$, where λ_{BR} is the Bychkov-Rashba parameter,[9] see also Ref. 23. Unlike in semiconductor heterostructures, the coupling in graphene does not depend on the magnitude of the electron momentum, as the electrons at $K(K')$ have a constant velocity. The electronic bands near $K(K')$ are now modified to

$$\varepsilon_{\mu\nu}=\mu\lambda_{BR}+\nu\sqrt{(\hbar v_F k)^2+(\lambda_{BR}-\mu\lambda_I)^2}. \quad (1)$$

The corresponding eigenvectors are

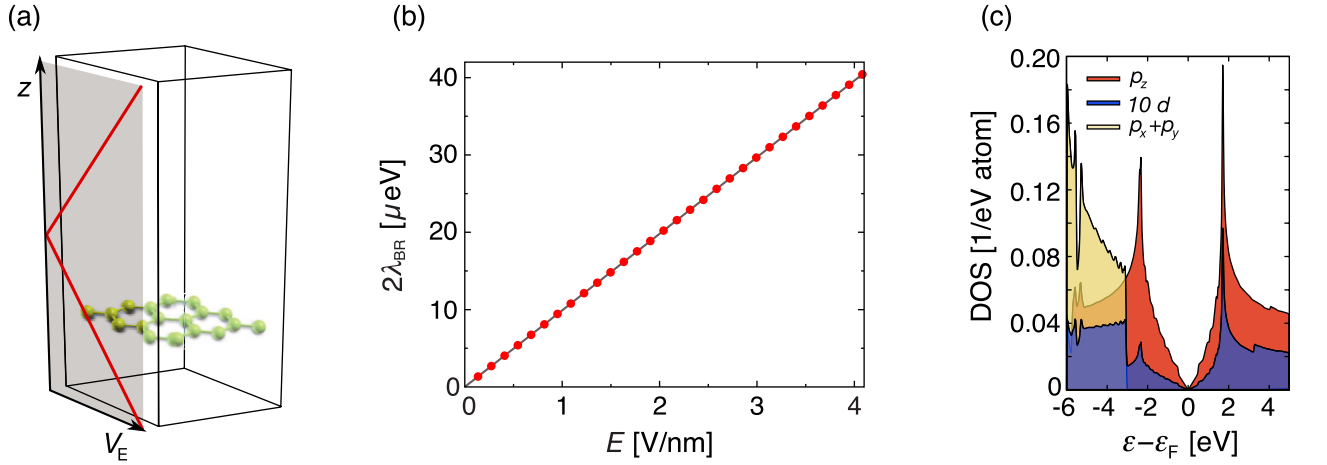

FIG. 3. (Color online) Bychkov-Rashba-type splitting in graphene and orbital-resolved density of states. (a) Transverse electric field is modeled with a zigzag potential. (b) Bychkov-Rashba spin-orbit induced splitting at $K(K')$ as a function of the electric field. The slope is 9.9 μeV per V/nm. (c) Projected density of states to particular atomic orbitals. The Fermi level is at zero. The d-character is enhanced by a factor of ten.

$$\psi_{\mu\nu} = (\chi_-|\kappa e^{-i\kappa\varphi}[(\varepsilon_{\mu\nu}-\lambda_I)/\varepsilon_0]^\kappa,\ 1\rangle + \mu\chi_+|-i\kappa e^{-i(1+\kappa)\varphi},\ ie^{-i\varphi}[(\lambda_I-\varepsilon_{\mu\nu})/\varepsilon_0]^\kappa\rangle)/C_{\mu\nu}, \tag{2}$$

with the normalization constant $C_{\mu\nu}=\sqrt{2}(1+[(\lambda_I-\varepsilon_{\mu\nu})/\varepsilon_0]^{2\kappa})^{/2}$. The expectation value of the spin,

$$s_{\mu\nu} = \frac{\varepsilon_0}{\sqrt{\varepsilon_0^2+(\lambda_I-\mu\lambda_{BR})^2}}\begin{pmatrix}\sin\varphi\\ -\cos\varphi\\ 0\end{pmatrix}, \tag{3}$$

is k dependent and lies in the graphene plane. The inclusion of the extrinsic coupling lifts the twofold degeneracy of the bands. Only the time-reversal Kramers degeneracy remains, coupling states at K and K'.

Our first principles results show that the above effective Hamiltonian model gives a remarkably faithful description of graphene's band structure at $K(K')$. The comparison is shown in Fig. 2. The dispersions given by Eq. (1) differ from the numerical results by less than 5% up to ± 200 meV away from the Fermi level. With the parameters supplied by the first principles calculations the analytical model becomes highly accurate.

The extrinsic splitting $2\lambda_{BR}$ is extracted as $(\varepsilon_{+-}-\varepsilon_{--})/2$ for $\lambda_{BR}<\lambda_I$, and $(\varepsilon_{++}-\varepsilon_{--})/2$ for $\lambda_{BR}>\lambda_I$, at K. Figure 3(a) illustrates the zigzag potential modeling the transverse field. The calculated $2\lambda_{BR}$ versus the electric field E is shown in Fig. 3(b). The dependence is linear with the slope of 10 μ eV nm/V. Since the field of 1 V/nm is produced by an electron charge 1 nm away from the graphene sheet, such fields are typical for graphene on a substrate. We expect that in realistic situations the intrinsic and extrinsic spin-orbit couplings compete, making the topologies described in Fig. 2 likely occurring in real samples. Since the extrinsic coupling depends linearly on the electric field, the topology is tunable by gates. We also give the calculated magnitude of the graphene's dipole moment (the shift of the electron charge density): 0.0134 CÅ in unit cell. One may then relate the Bychkov-Rashba effect directly to the induced dipolar moment; this should be particularly useful for estimating the extrinsic splitting due to adatoms absorption on graphene.

Previous numerical estimates for the intrinsic splitting $2\lambda_I$ in graphene are rather controversial. The splitting was estimated to be in the range of 1 to 200 μeV.[9,24–27] Kane and Mele[9] estimated the splitting of 200 μeV. This optimistic estimate was drastically reduced by Min *et al.*[24] to the value of 1 μeV, supported by subsequent works.[25,26] None of these studies were fully first principles. A density functional calculation of Boettger and Trickey,[27] using a Gaussian-type orbital fitting function methodology, gave 50 μeV. Our result is about one half of that; the difference is likely due to the different approximation schemes for spin-orbit coupling used in Ref. 27 and by us.[28] Previous estimates for the extrinsic splitting, $2\lambda_{BR}$, are 0.516 μeV (Ref. 9) and 133 μeV (Ref. 24) per V/nm. No fully first principles calculation of $2\lambda_{BR}$ or the extrinsic effects in graphene in general, was reported thus far.

What is the origin of the rather large, as compared to previous non fully first principles results, intrinsic spin-orbit splitting in graphene? We calculate the spin-orbit coupling splitting of the $2p$ levels in carbon atoms to be 8.74 meV, using the *Wien2k* code. This splitting should be reflected in the splitting of the bands at the Γ point. Our calculation finds the splitting at the Γ point of 8.978 meV about 3 eV below the Fermi level, in close agreement with the atomic value. The bands at the $K(K')$ points are formed mainly by p_z orbitals whose magnetic quantum number is zero. The intrinsic splitting can be due to the coupling of the p_z orbitals (forming the π bands) to either σ bands or bands formed by higher orbitals $(d,f,\ldots)$. As argued already by Slonczewski[17] using group theory, it is the d and higher orbitals that dominate the spin-orbit splitting at $K(K')$. A qualitative argument for that was provided by McClure and Yafet:[16] orbitals d_{xz} and d_{yz} can form Bloch states of the π band symmetry at $K(K')$. Due to a finite overlap between the neighboring p_z and d_{xz},d_{yz} orbitals, the intrinsic splitting is linearly proportional to the

spin-orbit splitting of the d states (orbitals higher than d have a smaller overlap and contribute less). In contrast, due to the absence of the direct overlap between the p_z and σ-band orbitals, the usually considered[9,24–26] spin-orbit splitting induced by the σ-π mixing depends only quadratically on the atomic spin-orbit splitting, giving a negligible contribution.

In Fig. 3(c) we show the orbital-resolved densities of states. The p_x, p_y atomic character vanishes above −3 eV (the Fermi level ε_F is at zero). The density of states close to ε_F comes predominantly from p_z orbitals (π bands). Nevertheless, there is a finite contribution from d orbitals (d_{xz} and d_{yz}) which follows in shape that of p_z. The contributions from $d_{x^2-y^2}$, d_{xy}, and d_{z^2} vanish for energies above the −3 eV. To further confirm the symmetry arguments of Slonczewski, we have selectively removed orbitals from the calculation of the spin-orbit coupling contribution. Removing d and higher orbitals reduces the intrinsic splitting to 0.98 μeV, reproducing earlier nonfirst principles calculations.[24–26] We conclude that the intrinsic splitting is dominated by d and higher orbitals, giving more than 96% of the splitting.[29] In contrast, we find that the extrinsic BR coupling is largely unaffected by the presence of d and higher orbitals, demonstrating that this coupling is due to the σ-π mixing.

Finally, we calculate the spin-orbit splitting for what we call a "miniripple" configuration (Fig. 4), in which every other atom is displaced by an amount Δ transverse to the sheet. This calculation should give an indication of what to expect for larger-scale ripples that occur in graphene on a substrate[30] or free standing;[31] such large scales are out of the scope for our methods. The miniripple exhibits a gap that grows quadratically with increasing Δ, as seen from Fig. 4.

Removing d and higher orbitals from the calculation of the spin-orbit splitting, the initial gap reduces to about 1 μeV but the overall growth remains largely unchanged: the rippling-induced gap is almost solely due to σ-π mixing. Furthermore, the displacements of less than 1% have no significant effects on the intrinsic spin-orbit splitting. For an effective description of the gap opening in the miniripple we consider a more general extrinsic case. The contribution of a transverse electric field is twofold. First, there is a pseudospin splitting, as the two sublattices are no longer equivalent (the two triangular sublattices have a different potential). Second, the Bychkov-Rashba effect appears. We find that the following formula describes the resulting spectrum: $\epsilon^K_{\mu\nu} = \nu\lambda_I + \mu[\delta_{1\nu}\lambda_\Delta + \delta_{-1\nu}\sqrt{\lambda_\Delta^2 + (2\lambda_{BR})^2}]$, where λ_Δ is the electric field induced gap due to the rippling ($\lambda_\Delta \propto E$).

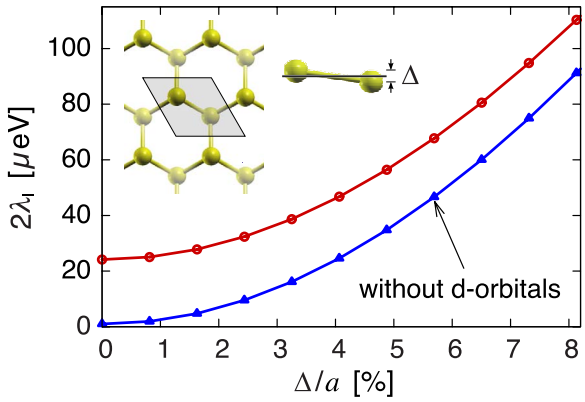

FIG. 4. (Color online) Calculated spectral gap at $K(K')$ in the miniripple configuration (inset), as a function of the relative corrugation strain with respect to the lattice constant a. Neglecting d and higher orbitals results in an almost constant shift, proving that the main effects come from σ-π hybridization.

In summary, we have shown that for realistic electric fields the graphene band structure exhibits remarkable tunable topologies. Our first-principles calculation gives strong support for the effective spin-orbit coupling Hamiltonian models, making them highly accurate analytical tools to investigate the physics of graphene.

We thank A. Matos-Abiague, P. Blaha, S. B. Trickey, and the *Wien2k* community for useful hints and discussions. This work was supported by the DFG Grants No. SFB 689 and No. SPP 1285. C.A.D. appreciates support from the Austrian Science Fund under Project No. I107.

[1] K. S. Novoselov, A. K. Geim, S. V. Morozov, D. Jiang, Y. Zhang, S. V. Dubonos, I. V. Grigorieva, and A. A. Firsov, Science **306**, 666 (2004).
[2] K. S. Novoselov, A. K. Geim, S. V. Morozov, D. Jiang, M. I. Katsnelson, I. V. Grigorieva, S. V. Dubonos, and A. A. Firsov, Nature (London) **438**, 197 (2005).
[3] Y. Zhang, Y.-W. Tan, H. L. Stormer, and P. Kim, Nature (London) **438**, 201 (2005).
[4] A. Bostwick, T. Ohta, T. Seyller, K. Horn, and E. Rotenberg, Nat. Phys. **3**, 36 (2007).
[5] A. K. Geim and K. S. Novoselov, Nature Mater. **6**, 183 (2007).
[6] S. Adam, E. H. Hwang, V. M. Galitski, and S. Das Sarma, Proc. Natl. Acad. Sci. U.S.A. **104**, 18392 (2007).
[7] A. H. Castro Neto, F. Guinea, N. M. R. Peres, K. S. Novoselov, and A. K. Geim, Rev. Mod. Phys. **81**, 109 (2009).
[8] N. Tombros, C. Jozsa, M. Popinciuc, H. T. Jonkman, and B. J. van Wees, Nature (London) **448**, 571 (2007).
[9] C. L. Kane and E. J. Mele, Phys. Rev. Lett. **95**, 226801 (2005).
[10] B. Trauzettel, D. V. Bulaev, D. Loss, and G. Burkard, Nat. Phys. **3**, 192 (2007).
[11] P. R. Wallace, Phys. Rev. **71**, 622 (1947).
[12] C. A. Coulson and R. Taylor, Proc. Phys. Soc. A **65**, 815 (1952).
[13] W. M. Lomer, Proc. R. Soc. Lond. **A227**, 330 (1955).
[14] J. W. McClure, Phys. Rev. **108**, 612 (1957).
[15] J. C. Slonczewski and P. R. Weiss, Phys. Rev. **109**, 272 (1958).
[16] J. W. McClure and Y. Yafet, *Proceedings of the Fifth Conference on Carbon* (Pergamon, New York, 1962), Vol. 1, pp. 22–28.
[17] J. C. Slonczewski, Ph.D. thesis, Rutgers University of New Jersey, 1955.
[18] P. Blaha, K. Schwarz, G. Madsen, D. Kvasnicka, and J. Luitz, *WIEN2k—An Augmented Plane Wave Plus Local Orbitals Program for Calculating Crystal Properties* (TU Wien, Austria,

2008).
[19] J. P. Perdew, K. Burke, and M. Ernzerhof, Phys. Rev. Lett. **77**, 3865 (1996).
[20] J. Stahn, U. Pietsch, P. Blaha, and K. Schwarz, Phys. Rev. B **63**, 165205 (2001).
[21] J. Fabian, A. Matos-Abiague, C. Ertler, P. Stano, and I. Žutić, Acta Phys. Slov. **57**, 565 (2007).
[22] Y. A. Bychkov and E. I. Rashba, JETP Lett. **39**, 78 (1984).
[23] E. I. Rashba, Phys. Rev. B **79**, 161409(R) (2009).
[24] H. Min, J. E. Hill, N. A. Sinitsyn, B. R. Sahu, L. Kleinman, and A. H. MacDonald, Phys. Rev. B **74**, 165310 (2006).
[25] Y. Yao, F. Ye, X.-L. Qi, S.-C. Zhang, and Z. Fang, Phys. Rev. B **75**, 041401(R) (2007).
[26] D. Huertas-Hernando, F. Guinea, and A. Brataas, Phys. Rev. B **74**, 155426 (2006).
[27] J. C. Boettger and S. B. Trickey, Phys. Rev. B **75**, 121402(R) (2007).
[28] The precise value of the intrinsic gap depends on the muffin-tin radius, since *Wien2k* calculates spin-orbit coupling only inside the muffin-tin sphere. (The present calculations use the maximum allowed sphere radius.) Although spin-orbit coupling is concentrated around the atom cores, making the inner-sphere approximation rather accurate, it is likely that the actual value of the gap is somewhat larger.
[29] The contribution to λ_I changes nonmonotonic as the maximum orbital state ℓ_{max} in the second variational scheme is increased. For $\ell_{max}=1$, 2, and 3 and more, we get $2\lambda_I \approx 1$, 26, and 24 μeV.
[30] M. Ishigami, J. H. Chen, W. G. Cullen, M. S. Fuhrer, and E. D. Williams, Nano Lett. **7**, 1643 (2007).
[31] A. Fasolino, J. H. Los, and M. I. Katsnelson, Nature Mater. **6**, 858 (2007).